Physical properties of the ferromagnetic heavy-fermion compound UIr$_2$Zn$_{20}$

E. D. Bauer,[1] A. D. Christianson,[1,2,3] J. S. Gardner,[4,5] V. A. Sidorov,[1,*] J. D. Thompson,[1] J. L. Sarrao,[1] and M. F. Hundley[1]

[1]*Los Alamos National Laboratory, Los Alamos, New Mexico 87545, USA*
[2]*Oak Ridge National Laboratory, Oak Ridge, Tennessee 37831, USA*
[3]*University of California, Irvine, California 92697, USA*
[4]*Indiana University, 2401 Milo B. Sampson Lane, Bloomington, Indiana 47408, USA*
[5]*NCNR, National Institute of Standards and Technology, Gaithersburg, Maryland 20899, USA*

Measurements of magnetization, specific heat, neutron diffraction, and electrical resistivity at ambient and applied pressure have been carried out on the cubic compound UIr$_2$Zn$_{20}$. A first-order-like ferromagnetic transition occurs at T_C=2.1 K with a saturation magnetization $\mu_{\text{sat}} \sim 0.4\mu_B$, indicating itinerant ferromagnetism. In this ordered state, the electronic specific heat coefficient remains large, $\gamma \sim 450$ mJ/mol K^2, classifying UIr$_2$Zn$_{20}$ as one of the very few heavy-fermion ferromagnets.

PACS number(s): 71.27.+a, 72.15.Qm

I. INTRODUCTION

Attention has been focused on uranium-based magnets to discern the nature of the strongly correlated electron ground state in these intermetallic compounds.[1] A rich variety of phenomena is found including the coexistence of unconventional superconductivity and magnetism,[2] pressure-induced superconductivity,[3] hidden order,[4] and non-Fermi-liquid behavior.[5] Of central importance in these uranium-based materials is the degree of localization of the 5f electrons. Various measurements on prototypical systems such as UPd$_2$Al$_3$ indicate a "dual nature" of the f electrons,[6] with two of three being localized and the remaining one itinerant. Recent work based upon a dual-nature model[7,8] of these strongly correlated electron materials show promise for making headway into this difficult electronic structure problem. Fortunately, Nature provides an abundance of intermetallic compounds to investigate spanning the entire range of localized/itinerant behavior, from truly localized, as revealed by large-moment magnetism (e.g., UGa$_2$)[9] or strong crystalline electric field excitations (e.g., UPd$_3$),[10] to itinerant magnets such as UGe$_2$ or UIr.[3,11] Yet another class of U-based heavy-fermion antiferromagnets possess an extremely large Sommerfeld coefficient $\gamma \sim 1$ J/mol K^2 suggesting a high degree of itinerancy at low temperatures, yet have reasonably large ordered moments ($\mu_{\text{ord}} \sim 1\mu_B$) indicating localized f-electron behavior.[12,13] Indeed, neutron scattering experiments on U$_2$Zn$_{17}$ reveal distinct responses characteristic of both itinerant and localized f electrons.[14] It is, therefore, worthwhile to search for other uranium compounds that exhibit "dual-nature" behavior.

A new family of lanthanide and actinide intermetallic compounds RX_2Zn$_{20}$ (R=lanthanide, Th, U; X=transition metal),[15–18] would appear, at first glance, to be ideal candidates for investigating magnetism and strong electronic correlations. These materials crystallize in the cubic Mg$_3$Cr$_2$Al$_{18}$ structure with an R-R spacing of more than 6 Å. This distance is considerably larger than the Hill limit[19] for U ($d_{\text{U-U}}^{\text{Hill}}$=3.5 Å) which roughly delineates two classes of actinide materials, one in which there is significant overlap of the actinide orbitals resulting in itinerant (paramagnetic)

f-electron behavior ($d_{\text{U-U}}^{\text{Hill}} < 3.5$ Å), and the other where there is negligible overlap leading to long-range magnetic order. While strong electronic correlations are manifest in the heavy-fermion behavior observed in the other UX_2Zn$_{20}$ (X=Fe, Ru; Co, Rh) compounds where the Sommerfeld coefficient ranges from 50 to 250 mJ/mol K^2, only UIr$_2$Zn$_{20}$ orders magnetically. The physical properties of UX_2Zn$_{20}$ (X=Fe, Ru; Co, Rh) will be reported elsewhere;[17,18] here, we focus on the behavior of UIr$_2$Zn$_{20}$.

We present measurements of neutron diffraction, specific heat, magnetization, and both magnetic susceptibility and electrical resistivity at applied pressure on the cubic compound UIr$_2$Zn$_{20}$. This material undergoes a first-order-like transition to a ferromagnetic state at 2.1 K. Within this state, a large electronic specific heat coefficient $\gamma \sim 450$ mJ/mol K^2 is observed. To our knowledge, UIr$_2$Zn$_{20}$ is the first truly heavy-fermion uranium-based ferromagnet discovered to date.

II. EXPERIMENTAL DETAILS

Single crystals AIr$_2$Zn$_{20}$ (A=Th, U) were grown in Zn flux.[20,21] The materials were placed in the ratio A:X:Zn =1:2:100 in a Ta crucible and sealed under vacuum in a quartz ampoule. The sample was heated to 600 °C for 12 h, then to 1050 °C for 4 h, followed by a slow cool at 4 °C/h to 700 °C, at which point the excess molten Zn flux was removed using a centrifuge.

Magnetic measurements were performed in magnetic fields up to 6.5 T from 1.8 to 300 K using a commercial superconducting quantum interference device magnetometer. Specific heat measurements were carried out in a commercial cryostat from 0.4 to 300 K using an adiabatic heat-pulse technique. Four-wire electrical resistivity were also performed in a commercial cryostat from 0.4 to 300 K. In some cases, the electrical resistivity measurements were performed in a small magnetic field was applied (H=0.2 T) to suppress impurity superconductivity from Zn inclusions.

Neutron powder diffraction data were collected using the BT-1 neutron powder diffractometer at the NIST Center for Neutron Research (NCNR). A Cu(311) monochromator pro-

TABLE I. Structural refinement of UIr_2Zn_{20} at 0.6 K. U_{iso} is defined as one-third of the trace of the orthogonalized U_{ij} tensor. Uncertainties in the last digit are enclosed in parentheses.

Space group $Fd\bar{3}m$				$a=14.1783(1)$ Å,	$V=2850.20(6)$ Å^3
(No. 227, origin choice 2, $Z=8$)				$\rho_{calc}=8.996$ gm/cm^3	
		Atomic positions			
Atom	Site	x	y	z	U_{iso} (10^2 Å^2)
U	8a	1/8	1/8	1/8	0.21(8)
Ir	16d	1/2	1/2	1/2	0.54(4)
Zn(1)	16c	0	0	0	1.14(10)
Zn(2)	48f	0.4860(2)	1/8	1/8	0.74(7)
Zn(3)	96g	0.0596(1)	0.0596(1)	0.3244(2)	0.70(4)
	Reduced $\chi^2=3.214$	$R_{wp}=13.04\%$	$R_p=10.42\%$		

duced neutrons with a wavelength $\lambda=1.5403(2)$ Å. Data were collected over the range of $2\theta=3-168°$ with a step size of 0.05°. A 5 g sample of UIr_2Zn_{20} was measured at 0.6 and 4.2 K for 8 h at each temperature in a single shot ^{3}He system.

Two high-pressure cells were used for the electrical resistivity measurements: a clamped piston cylinder and a toroidal anvil cell. The toroidal is a profiled anvil system supplied with a boron-epoxy gasket and Teflon capsule, containing pressure-transmitting liquid, sample and a pressure sensor.[22] The pressure in both cells was determined from the variation of the superconducting transition of lead using the pressure scale of Eiling and Schilling.[23] Both ac susceptibility and electrical resistivity measurements were carried out in a ^{4}He cryostat between 1 and 300 K using a commercial resistance bridge operating at 15 Hz with excitation currents ranging from 500 μA to 1 mA. Two samples were used in this study. Sample No. 1 was placed in the clamped pressure cell after the ambient pressure electrical resistivity measurements were completed. This sample was judged to have somewhat more free Zn content from the metallic behavior of the resistivity. Sample No. 2 was used for both the ac susceptibility and electrical resistivity measurements in the torodial cell. The behavior of both was qualitatively similar.

III. RESULTS AND DISCUSSION

Refinements of the neutron diffraction data yield good agreement with the $Mg_3Cr_2Al_{18}$ structure type.[15] In this ordered structure, the uranium atoms possess cubic symmetry and are located at the center of 16-fold coordinated Zn polyhedra. Likewise, the Ir atoms are situated within a Zn icosahedra. The lattice constant, atom positions, and isotropic thermal parameters are listed in Table I. All refinements yielded full occupancy of the atomic sites. We were unable to index several small peaks corresponding to an unknown impurity phase with a concentration of less than 3%.

The magnetic susceptibility $\chi(T)$ of UIr_2Zn_{20} is displayed in Fig. 1 measured in a magnetic field $H=0.1$ T. The data can be fit by a Curie-Weiss law above 100 K as shown in the inset (a) of Fig. 1, yielding an effective moment $\mu_{eff}=3.6\mu_B$, close to the value expected for either a $5f^2$ (μ_{eff}

$=3.58\mu_B$) or $5f^3$ ($\mu_{eff}=3.62\mu_B$) configuration, and a large (negative) Curie-Weiss temperature $\theta=-123$ K. Below 5 K, the magnetic susceptibility increases dramatically and an anomaly is observed at 2.75 K ($H=0.1$ T) consistent with a ferromagnetic phase transition. (As shown below, the magnetic transition temperature is quite sensitive to magnetic field and increases from $T_C=2.1$ K in zero field to 2.75 K in 0.1 T.)

Isothermal magnetization measurements at 2 and 10 K on UIr_2Zn_{20} shown in Fig. 2 confirm the onset of ferromagnetism slightly above 2 K. (An Arrott plot analysis,[24] i.e., extrapolation of $M^2 \to 0$ from a plot of M^2 vs H/M, is also consistent with this result.) A full hysteresis loop at 2 K is displayed in the inset of Fig. 2. Both the coercive field ($H_c \sim 12$ Oe) and the remnant magnetization ($M_R \sim 0.05\mu_B$) classify UIr_2Zn_{20} as a soft ferromagnet. A saturation magnetization of $M_{sat} \sim 0.4\mu_B$/U atom obtained from linear fit to the high field data ($H>4$ T) at 2 K indicates itinerant magnetism. An extrapolation of the $\chi(T)$ data assuming a Bloch law [$M=M_0(1-aT^{3/2})$] (Ref. 25) below the phase transition at 2.75 K in $H=0.1$ T yields a spontaneous magnetization $M_0=0.3\mu_B$; it is expected that the zero temperature value will not be too different from these values.
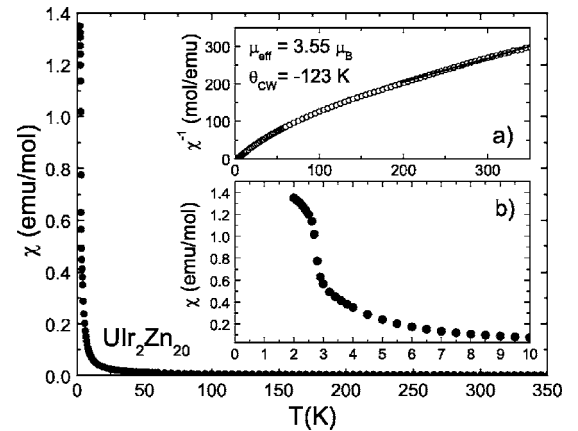

FIG. 1. Magnetic susceptibility $\chi(T)$ of UIr_2Zn_{20} at $H=0.1$ T. Inset: Inverse magnetic susceptibility $\chi^{-1}(T)$. The solid line is a linear fit to the data.
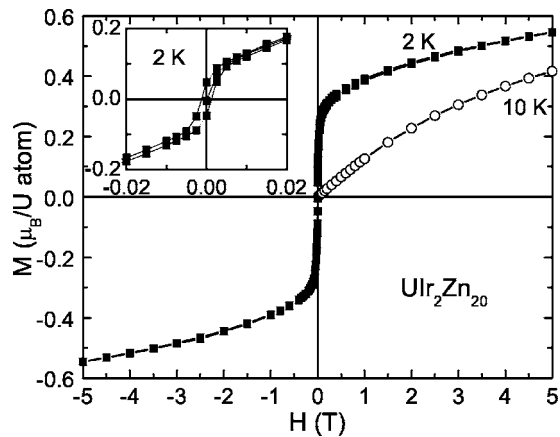
FIG. 2. Magnetization M of UIr$_2$Zn$_{20}$ at 2 K (solid squares) and 10 K (open circles). Inset: Hysteresis loop $M(H)$ at 2 K.

FIG. 3. Specific heat C/T vs T of UIr$_2$Zn$_{20}$ (solid squares) and ThIr$_2$Zn$_{20}$ (line) below 10 K. Inset: $\Delta C/T$ vs T (left axis) and S_{5f} (right axis).

Neutron diffraction measurements on UIr$_2$Zn$_{20}$ were employed to determine the nature of the magnetic phase transition at 2.1 K by directly comparing data collected at both 0.6 and 4.2 K. The data at 0.6 K do not show any additional intensity at either antiferromagnetic or ferromagnetic (coinciding with nuclear Bragg peaks) positions relative to the data at 4.2 K above the transition. Assuming a simple ferromagnetic model, the data are consistent with an upper bound of the magnitude of the magnetic moment of less than $1\mu_B$ (the neutron absorption of Ir precludes further refinement of this estimate), in agreement with the magnetization measurements (Fig. 2). However, the UIr$_2$Zn$_{20}$ sample was shown to depolarize a polarized beam of neutrons at 0.6 K, indicative of a ferromagnetic component to the low temperature phase. The similarity between the data above and below the phase transition at 2.1 K, including the goodness of fit, the lattice constants, and the atomic positions suggests there is no structural distortion associated with this transition. At this point, a large ferromagnetic component to a more complicated magnetic structure cannot be ruled out; further measurements are in progress to determine the exact nature of the magnetic transition in this material. For simplicity, we will continue to refer to it a ferromagnetic transition.

Figure 3 shows the specific heat, plotted as C/T vs T, of UIr$_2$Zn$_{20}$ and the isostructural compound ThIr$_2$Zn$_{20}$. A ferromagnetic transition is observed at $T_C=2.1$ K. Analysis of the heat-pulse decay curves does not reveal features characteristic of a strong first-order transition in specific heat;[26] however, the symmetry of the peak in C/T suggests the transition into the ferromagnetic state is weakly first order. After subtraction of the specific heat of nonmagnetic ThIr$_2$Zn$_{20}$, the $5f$ contribution to the specific heat $\Delta C/T$ is displayed in the inset of Fig. 3. $\Delta C/T$ increases monotonically below 10 K reaching a value ~ 450 mJ/mol K^2 at 2.5 K just before the onset of ferromagnetism. Within the ferromagnetic state, the $5f$ contribution remains large: a linear extrapolation below 0.4 K yields $\Delta C/T \sim 450$ mJ/mol K^2. The magnetic entropy $S_{5f}(2.5$ K$)\int(\Delta C/T)dT \sim 1.2$ J/mol K, implying itinerant ferromagnetism in UIr$_2$Zn$_{20}$, in agreement with the reduced moment determined from magnetization measurements described above. At 10 K, the entropy amounts to $S_{5f}=4$ J/mol K ~ 0.7R ln(2).
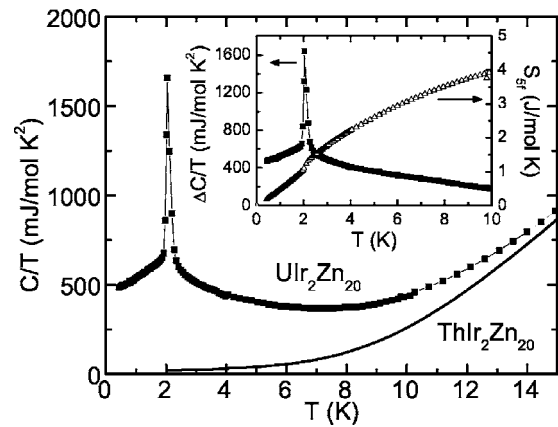
The $5f$ contribution to specific heat $\Delta C/T$ of UIr$_2$Zn$_{20}$ in magnetic fields up 9 T is shown in Fig. 4. The first-order-like transition at 2.1 K in zero field moves higher in temperature with increasing field for $H < 1.5$ T, then increases more slowly above 1.5 T as displayed in Fig. 5(a). Concomitant with this increase of the transition temperature, the phase transition evolves from first-order-like to more second-order-like for $H > 0.1$ T. There is a moderate suppression of the specific heat coefficient from $\gamma \sim 450$ mJ/mol K^2 at $H = 0$ T to ~ 250 mJ/mol K^2 at $H=9$ T as shown in Fig. 5(b). The magnetic entropy is shown in the inset of Fig. 4 (a linear extrapolation of the $\Delta C/T$ data below 0.4 K was used to obtain S_{5f}). The entropy released below T_C remains roughly constant at $S_{5f} \sim 1.2$–2.0 J/mol K in applied field despite the change in the shape of the transition above 0.1 T.

The electrical resistivity $\rho(T)$ of UIr$_2$Zn$_{20}$ is shown in Fig. 6. The room temperature value of ρ is 175 $\mu\Omega$ cm and $\rho_0 = 15$ $\mu\Omega$ cm, resulting in residual resistivity ratio (RRR) $= 12$. $\rho(T)$ is weakly temperature dependent at high temperatures, passes through a maximum at $T_{max} \sim 85$ K, and decreases more rapidly below ~ 50K. An obvious change in slope of $\rho(T)$ denotes the Curie temperature at $T_C=2.0$ K.
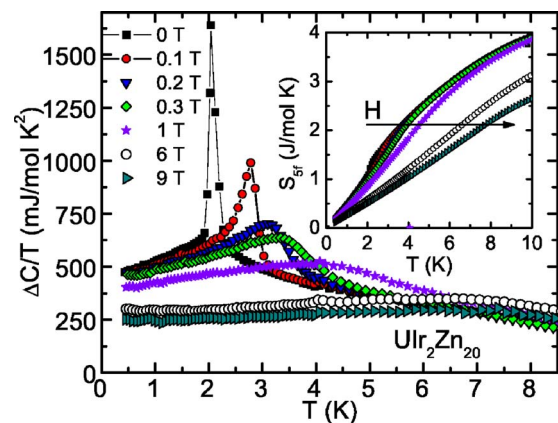

FIG. 4. (Color online) $5f$ contribution to the specific heat $\Delta C/T$ vs T of UIr$_2$Zn$_{20}$ in magnetic fields up to 9 T for $H\|[111]$. Inset: $S_{5f}(T)$ for $H \leqslant 9$ T.
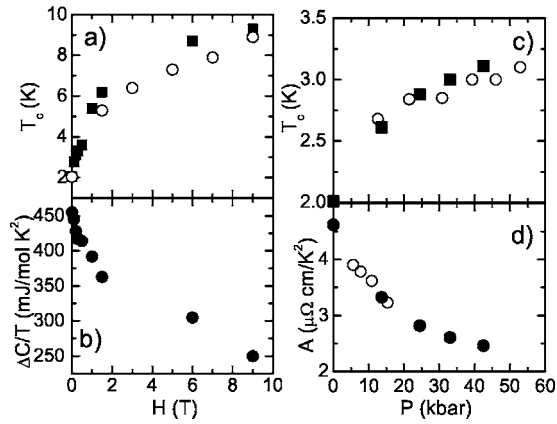
FIG. 5. Physical properties of UIr_2Zn_{20}. (a) Curie temperature $T_C(H)$ determined from specific heat (solid squares) and electrical resistivity (open circles), (b) $5f$ contribution to the specific heat $\Delta C/T$ vs H, (c) $T_C(P)$ determined from electrical resistivity (solid squares) and ac susceptibility (open circles) at various pressures up to 53 kbar on sample No. 2. (d) T^2 coefficient of resistivity $A(P)$ of sample No. 1 (open circles) and sample No. 2 (solid circles). The data at ambient pressure of sample No. 1 has been normalized to that of sample No. 2 for comparison.

With increasing magnetic field, the transition temperature moves to higher temperature, in agreement with the specific heat measurements discussed above. Below T_C, a Fermi-liquid T^2 temperature dependence of $\rho(H,T)$ is observed. Fits of the data to $\rho=\rho_0+AT^2$ yield a monotonically decreasing A coefficient with applied field (not shown). The Kadowaki-Woods relation[27] $[A/\gamma^2=1\times10^{-5} \mu\Omega$ cm $(mol K/mJ)^2]$ implies an electronic specific heat coefficient $\gamma=600$ mJ/mol K^2 for $H=0$ and 220 mJ/mol K^2 at $H=9$ T, comparable to the values determined from specific heat measurements. In a simplified model of the sharp Abrikosov-Suhl resonance at the Fermi level E_F in the Kondo picture,[28] the application of a magnetic field will broaden the resonance (whose width is proportional to the Kondo temperature T_K) and, hence, further populate
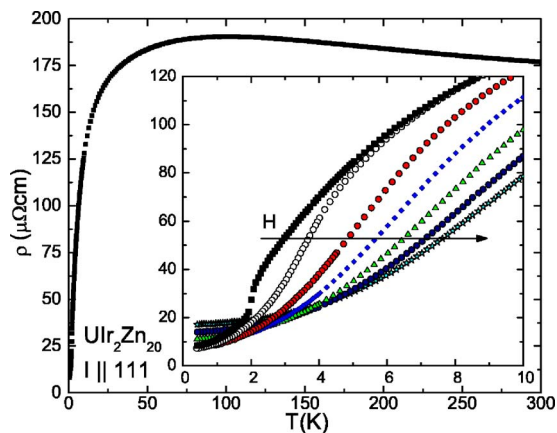

FIG. 6. (Color online) Electrical resistivity $\rho(T)$ of UIr_2Zn_{20} below 300 K for $I\|111$. Inset: $\rho(T)$ below 10 K in magnetic fields up to $H=9$ T. From left to right the fields are 0, 0.3, 1.5, 3, 5, 7, and 9 T.
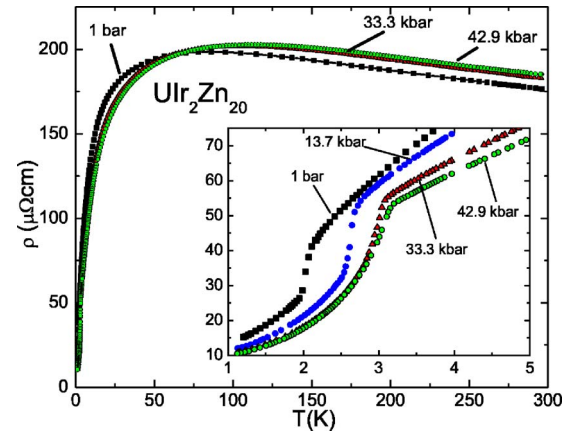

FIG. 7. (Color online) Electrical resistivity $\rho(T)$ of UIr_2Zn_{20} (sample No. 2) at various pressures up to 43 kbar. Inset: $\rho(P,T)$ below 5 K.

the lower spin-up band. This leads to an increase in T_K and, hence, a decrease in γ ($\propto 1/T_K$), as is observed experimentally [Figs. 4 and 5(b)]. No superconductivity is observed above 0.4 K. It is known that unconventional superconductivity coexisting with ferromagnetism in such materials as URhGe is extremely sensitive to disorder,[29] which may account for the lack of superconductivity in UIr_2Zn_{20}.

The electrical resistivity $\rho(T)$ on sample No. 2 of UIr_2Zn_{20} at various pressures up to $P=43$ kbar is displayed in Fig. 7. The application of pressure does not significantly change the overall shape and magnitude of the $\rho(T)$ curves—a result not unexpected given the relative isolation of both the uranium and iridium atoms in this structure. The Curie temperature increases with applied pressure (inset of Fig. 7) at a rate $dT_C/dP=0.04$ K/kbar up to 25 kbar then increases more slowly for $P>25$ kbar as shown in Fig. 5(c). At modest pressures below 13 kbar, the shape of $d\rho/dT$ is reminiscent of a first-order phase transition (not shown); above 13 kbar, $d\rho/dT$ acquires the characteristic shape of a second-order transition in specific heat.[30] Fits of the data within the magnetic state to a T^2 temperature dependence reveal decrease of the A coefficient with applied pressure as shown in Fig. 5(d). [The data can also be reasonably well described by $\rho-\rho_0=BT^n$ with $n=2.5$ (not shown).] The increase of the temperature of the maximum in $\rho(P,T)$, T_{max}, and the concomitant decrease of A with applied pressure implies that the Kondo temperature increases with P, similar to a number of other Ce- and U-based heavy-fermion materials.[31] Both the increase of the Curie temperature and the decrease in the A coefficient with applied pressure, and the large electronic specific heat coefficient suggests that UIr_2Zn_{20} is located just to the left of the maximum in the Doniach diagram.[32] The ac-susceptibility measurements on sample No. 2 up to 53 kbar are displayed in Fig. 8; the Curie temperatures deduced from these curves are in excellent agreement with those determined from electrical resistivity [Fig. 5(d)].

UIr_2Zn_{20} displays all the characteristics of a heavy-fermion ferromagnet. At high temperatures, the f-electron magnetic moments are only weakly hybridized with the conduction electrons and remain localized, as evidenced by a
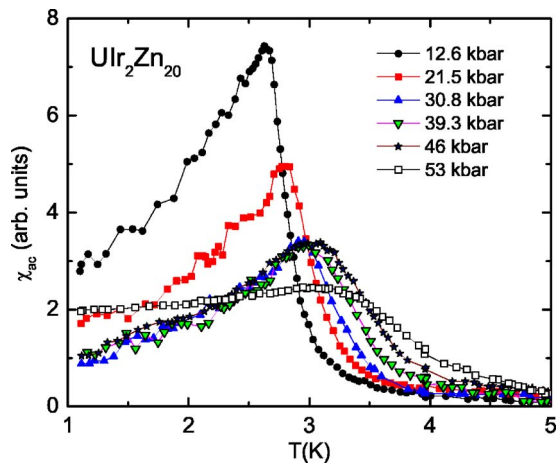
FIG. 8. (Color online) Real part of the ac magnetic susceptibility $\chi_{ac}(T)$ of UIr_2Zn_{20} (sample No. 2) at various pressures up to P = 53 kbar.

FIG. 9. (Color online) Rhodes-Wohlfarth plot μ_{eff}/μ_{sat} vs T_C, for various materials.

Curie-Weiss susceptibility (Fig. 1). As the temperature is lowered, the system evolves continuously to a heavy Fermi-liquid ground state where the f-electrons appear to be itinerant; in this case, ferromagnetism intervenes before this zero temperature Fermi-liquid state is reached. The zero-temperature γ in heavy-fermion antiferromagnets such as U_2Zn_{17} and UCd_{11}[13] is approximately 1/3 of the value at the ordering temperature implying that some of the (itinerant) heavy quasiparticles are removed from the Fermi surface in the ordered state; a similar factor of 1/3 appears when comparing the ratio of the ordered and effective moments [or equivalently, the remaining mean-square fluctuating moment $(\mu_{eff}^2 - \mu_{ord}^2)/\mu_{ord}^2$].[33] It is interesting to note this "1/3" rule holds true for many U-based heavy-fermion magnets, despite their different antiferromagnetic structures.[13] The ferromagnetic transition UIr_2Zn_{20} probably results in a simple magnetic structure in this cubic material and, hence, does not drastically alter the Fermi surface upon ordering; this may be one reason for the near equality of the Sommerfeld coefficient above and below T_C. While this small change in γ on either side of the transition is not unexpected if it is first-order-like, it is unusual, at least compared to other heavy-fermion antiferromagnets, that such behavior is observed when the phase transition appears to be second-order for $H > 0.1$ T. In addition, upon entry into the ferromagnetic state, the heavy band(s) of UIr_2Zn_{20} associated with the heavy-fermion state that begin(s) to develop above T_c will split into spin-up and spin-down bands. However, this splitting will be small (of order $T_C = 2$ K); hence, there will be little effect on the heavy quasiparticle formation within the ferromagnetic state. In contrast, the larger internal magnetic field in the antiferromagnets such as UCd_{11} may have a greater effect on the narrower peak in the density of states ($\gamma \sim 800$ mJ/mol/K^2) than in UIr_2Zn_{20}. It is difficult to determine the degree of localization in UIr_2Zn_{20}; further measurements on UIr_2Zn_{20} are necessary to compare it to other heavy-fermion compounds such as U_2Zn_{17} or UPd_2Al_3 in which a variety of experiments indicate 2 of the 3 U f electrons are localized.[6,14]

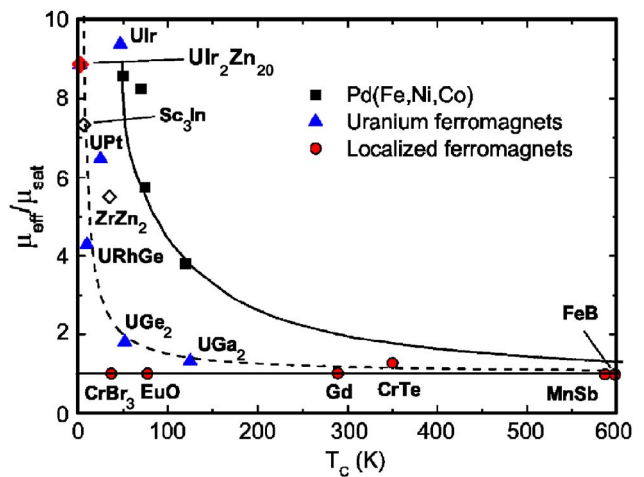To place UIr_2Zn_{20} within the context of other itinerant ferromagnets, it is useful to construct a Rhodes-Wholfarth plot,[34,35] i.e., the ratio of effective and saturation moments μ_{eff}/μ_{sat} vs T_C, as shown in Fig. 9. The U-based itinerant ferromagnets [e.g., URhGe (Ref. 29), UPt (Ref. 36)] have much lower Curie temperatures than the $3d$ ferromagnets involving dilute magnetic impurities in Pd, consistent with a narrow f band at the Fermi level.[34] UIr_2Zn_{20} has a large value of $\mu_{eff}/\mu_{sat} = 8.9$, comparable to the ferromagnetic, pressure-induced superconductor UIr but with an order of magnitude smaller Curie temperature.[11,37] Such a large value of μ_{eff}/μ_{sat} suggests predominantly itinerant f-electron character, in marked contrast to the localized ferromagnets (e.g., UGa_2) in which $\mu_{eff}/\mu_{sat} \sim 1$.[34]

In summary, the physical properties of UIr_2Zn_{20} have been measured by means of neutron diffraction, magnetization, specific heat, and electrical resistivity and ac susceptibility under pressure. This material undergoes a phase transition to a ferromagnetic state below $T_C = 2.1$ K. Specific heat measurements indicate the Sommerfeld coefficient is $\gamma \sim 450$ mJ/mol K^2 within the ferromagnetic state, classifying it as a heavy-fermion material. Further neutron diffraction measurements are planned to determine the magnetic structure of UIr_2Zn_{20}, while other measurements including photoemission are in progress to further probe the degree of localization itinerancy in this interesting material.

*Also at: Institute for High Pressure Physics, Russian Academy of Sciences, 142190 Troitsk, Russia.

[1] V. Sechovský and L. Havela, in *Ferromagnetic Materials*, edited by E. P. Wohlfarth and K. H. J. Buschow (North-Holland, Amsterdam, 1988), Vol. 4, p. 309.

[2] C. Geibel, C. Schank, F. Jährling, B. Buschinger, A. Grauel, T. Lühman, P. Gegenwart, R. Helfrich, P. H. P. Reinders, and F. Steglich, Physica B **199–200**, 128 (1994).

[3] S. S. Saxena, P. Agarwal, K. Ahllan, F. M. Grosche, R. K. W. Haselwimmer, M. J. Steiner, E. Pugh, I. R. Walker, S. R. Julian, P. Monthoux, G. G. Lonzarich, A. Huxley, I. Sheikin, D. Braithwaite, and J. Flouquet, Nature (London) **406**, 587 (2000).

[4] H. Amitsuka, M. Sato, N. Metoki, M. Yokoyama, K. Kuwahara, T. Sakakibara, H. Morimoto, S. Kawarazaki, Y. Miyako, and J. A. Mydosh, Phys. Rev. Lett. **83**, 5114 (1999); M. Jaime, K. H. Kim, G. Jorge, S. McCall, and J. A. Mydosh, *ibid.* **89**, 287201 (2002); P. Chandra, P. Coleman, J. A. Mydosh, and V. Tripathi, Nature (London) **417**, 831 (2002).

[5] E. D. Bauer, V. S. Zapf, P.-C. Ho, N. P. Butch, E. J. Freeman, C. Sirvent, and M. B. Maple, Phys. Rev. Lett. **94**, 046401 (2005).

[6] H. Sato, Y. Abe, H. Okada, T. D. Matsuda, K. Abe, H. Sugawara, and Y. Aoki, Phys. Rev. B **62**, 15125 (2000).

[7] G. Zwicknagl and P. Fulde, J. Phys.: Condens. Matter **15**, S1911 (2003).

[8] D. V. Efremov, N. Hasselmann, E. Runge, P. Fulde, and G. Zwicknagl, Phys. Rev. B **69**, 115114 (2004).

[9] A. V. Andreev, K. P. Belov, A. V. Deriagin, R. Z. Levitin, and A. Menovsky, J. Phys. (Paris), Colloq. **40**, C4 (1979).

[10] W. J. L. Buyers, A. F. Murray, T. M. Holden, E. C. Svensson, P. Plessis, G. H. Lander, and O. Vogt, Physica B & C **102**, 291 (1980).

[11] T. Akazawa, H. Hidaka, T. Fujiwara, T. C. Kobayashi, E. Yamamoto, Y. Haga, R. Settai, and Y. Onuki, J. Phys.: Condens. Matter **16**, L29 (2004).

[12] Z. Fisk, J. D. Thompson, and H. R. Ott, J. Magn. Magn. Mater. **76&77**, 637 (1988).

[13] H. R. Ott and Z. Fisk, in *Handbook on the Physics and Chemistry of the Actinides*, edited by A. J. Freeman and G. H. Lander (North-Holland, Amsterdam, 1987), Vol. 5, Chap. 2, p. 85.

[14] C. Broholm, J. K. Kjems, G. Aeppli, Z. Fisk, J. L. Smith, S. M. Shapiro, G. Shirane, and H. R. Ott, Phys. Rev. Lett. **58**, 917 (1987).

[15] A. P. Goncalves, J. C. Waerenborgh, A. Amaro, M. Godinho, and M. Almeida, J. Alloys Compd. **271–273**, 456 (1998).

[16] S. Jia, S. L. Bud'ko, G. D. Samolyuk, and P. C. Canfield, cond-mat/0606615 (unpublished).

[17] E. D. Bauer, A. Silhanek, F. Ronning, D. Garcia, N. Harrison, J. D. Thompson, A. Lobos, A. A. Aligia, J. L. Sarrao, R. Movshovich, M. F. Hundley, and M. Jaime (unpublished).

[18] M. S. Torikachvili, S. Jia, S. T. Hannahs, R. C. Black, W. K. Neils, Dinesh Martien, S. L. Bud'ko, and P. C. Canfield, cond-mat/0608422 (unpublished).

[19] H. H. Hill, in *Plutonium and Other Actinides*, edited by W. N. Miner (AIME, New York, 1970), p. 2.

[20] Z. Fisk and J. P. Remeika, in *Handbook on the Physics and Chemistry of the Rare Earths*, edited by K. A. Gschneidner, Jr. and L. Eyring (North-Holland, Amsterdam, 1989), Vol. 12, Chap. 81, p. 53.

[21] P. C. Canfield and Z. Fisk, Philos. Mag. B **65**, 1117 (1992).

[22] L. G. Khvostantsev, V. A. Sidorov, and O. B. Tsiok, in *Properties of Earth and Planetary Materials at High Pressures and Temperatures, Geophysical Monograph 101*, edited by H. Manghnani and T. Yagi (American Geophysical Union, Washington, D.C., 1998), p. 89.

[23] A. Eiling and J. S. Schilling, J. Phys. F: Met. Phys. **11**, 623 (1981).

[24] A. Arrott, Phys. Rev. **108**, 1394 (1957).

[25] See, for example, C. Kittel, *Quantum Theory of Solids* (Wiley, New York, 1963), p. 56.

[26] J. Lashley, M. F. Hundley, A. Migliori, J. L. Sarrao, P. G. Pagliuso, T. W. Darling, M. Jaime, J. C. Cooley, W. L. Hults, L. Morales, D. J. Thoma, J. L. Smith, J. Boerio-Goates, B. F. Woodfield, G. R. Stewart, R. A. Fisher, and N. E. Phillips, Cryogenics **43**, 369 (2003).

[27] K. Kadowaki and S. B. Woods, Solid State Commun. **58**, 307 (1986).

[28] K. D. Schotte and U. Schotte, Phys. Lett. **55A**, 38 (1975).

[29] Y. Aoki, T. Namiki, S. Ohsaki, S. R. Saha, H. Sugawara, and H. Sato, J. Phys. Soc. Jpn. **71**, 2098 (2002).

[30] M. E. Fisher and J. S. Langer, Phys. Rev. Lett. **20**, 665 (1968).

[31] J. D. Thompson and J. M. Lawrence, in *Handbook on the Physics and Chemistry of the Rare Earths*, edited by K. A. Gschneidner, Jr., L. Eyring, G. H. Lander, and G. R. Choppin (North-Holland, Amsterdam, 1994), Vol. 19, Chap. 133, p. 383.

[32] S. Doniach, Physica B & C **91**, 231 (1977).

[33] G. Aeppli, Physica B **318**, 5 (2002).

[34] P. R. Rhodes and E. P. Wohlfarth, Proc. R. Soc. London **273**, 247 (1963).

[35] E. P. Wohlfarth, J. Magn. Magn. Mater. **7**, 113 (1978).

[36] B. T. Matthias, C. W. Chu, E. Corenzwit, and D. Wohlleben, Proc. Natl. Acad. Sci. U.S.A. **64**, 459 (1969).

[37] E. D. Bauer, E. J. Freeman, C. Sirvent, and M. B. Maple, J. Phys.: Condens. Matter **13**, 5675 (2001).